# ON THE PERFORMANCES OF DIFFERENT TYPES OF CONTROLLERS FOR ACTIVE POWER FILTERS

**Mihai CULEA**

*"Dunărea de Jos" University of Galați*
*Advanced Control Systems Research Center*
111, Domnească, 800201-Galați, Romania

Abstract: This paper analyses the performances of three different types of controllers for shunt active power filters. The controllers are used in the d-q frame, the same frame in which the reference signal for the 5th and 7th harmonics is injected. Performance is evaluated based on amplitude and phase error between the injected reference and the output of the active power filter.

Keywords: Active Power Filter; Controllers;

## 1. INTRODUCTION

The harmonic problem in the power systems has received increased attention in recent years. The large scale use of semiconductor switching devices and the proliferation of nonlinear loads have led to an high level of harmonics and other power quality related problems [1], [2], [3].

Tuned passive filters (PF) have been used to mitigate harmonics but their performance depends on the system and they can resonate with system impedance in some cases [4]. Moreover, the PF are bulky and degenerate with age. To overcome these drawbacks several types of shunt active power have been investigated and used to eliminate harmonics and compensate reactive power [5], [6].

The structure of a shunt APF is presented in Fig.1. Basically, the APF is acting as a shunt for the harmonic currents from the mains. The performance of APF depends on two key issues: one is the detection of harmonic currents and the other is the control of compensating currents for APF to track the reference currents.

This paper will address the second issue and the performance of the controllers will be evaluated based on the amplitude and phase error between the reference signal and the output of the APF.

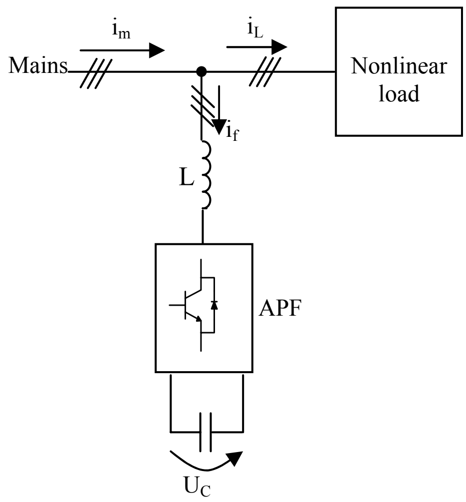


Fig.1. Active power filter – APF

A reference signal corresponding to 5th and 7th harmonics will be used to test the controllers. The control scheme used is presented in Fig.2 and it uses the d-q currents control [7], [8].

Three different types of controllers were used: a PI controller, a PI lead-lag and a PI+resonant controller.

The paper is organized as follows. The method for injecting harmonics in the d-q frame is presented in section 2.

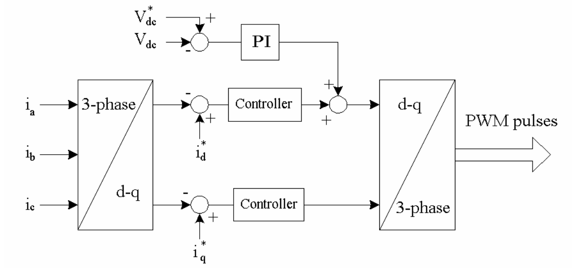


Fig.2. Control scheme for the APF

The characteristics of the controllers used in the control scheme are presented in section 3. Some simulation results as well as practical results are presented in section 4 and the comparison between the controllers is made in section 5. Some concluding remarks end this paper.

## 2. HARMONICS INJECTION IN THE D-Q PLANE

In the case of the active power filters the harmonics to be controlled are the $6k \pm 1$ rank harmonics. In order to inject these harmonics their image in the d-q frame was first determined. Considering a three-phase currents system, which has the 5th harmonic besides the fundamental, this can be written as:

$$(1)\quad \begin{aligned} i_a(t) &= I\cos(\theta) + I_5\cos(5\theta+\varphi_5) \\ i_b(t) &= I\cos\left(\theta-\frac{2\pi}{3}\right) + I_5\cos\left(5\theta+\varphi_5+\frac{2\pi}{3}\right) \\ i_c(t) &= I\cos\left(\theta+\frac{2\pi}{3}\right) + I_5\cos\left(5\theta+\varphi_5-\frac{2\pi}{3}\right) \end{aligned}$$

where I – amplitude of the fundamental, $I_5$ – amplitude of the 5th harmonic, $\theta = \omega t$, $\varphi_5$ – phase angle of the 5th harmonic.

Applying the Clarke transform to the three-phase currents system the α-β currents are:

$$(2)\quad \begin{aligned} i_\alpha &= \frac{3}{2}i_a = \frac{3}{2}\big(I\cos(\theta)+I_5\cos(5\theta+\varphi_5)\big) \\ i_\beta &= \frac{\sqrt{3}}{2}(i_b - i_c) = \frac{\sqrt{3}}{2}\left(I\cos\left(\theta-\frac{2\pi}{3}\right) - I_5\cos\left(5\theta+\frac{2\pi}{3}+\varphi_5\right)\right) - \\ &-\frac{\sqrt{3}}{2}\left(I\cos\left(\theta+\frac{2\pi}{3}\right)+I_5\cos\left(5\theta-\frac{2\pi}{3}+\varphi_5\right)\right) \end{aligned}$$

In the d-q frame the currents can be written as:

$$(3)\quad \begin{aligned} i_d &= \frac{2}{3\sqrt{2}}\big(i_\alpha\cos(\theta)+i_\beta\sin(\theta)\big) \\ &= \frac{1}{\sqrt{2}}[\big(I\cos^2(\theta)+I_5\cos(5\theta+\varphi_5)\cos(\theta)\big)+I\sin^2(\theta) - \\ &-I_5\sin(5\theta+\varphi_5)\sin(\theta)] \\ &= \frac{1}{\sqrt{2}}\big(I+I_5\cos(6\theta+\varphi_5)\big) \end{aligned}$$

and:

$$(4)\quad \begin{aligned} i_q &= \frac{2}{3\sqrt{2}}\big(i_\beta\cos(\theta)-i_\alpha\sin(\theta)\big) \\ &= \frac{1}{\sqrt{2}}[\big(I\sin(\theta)\cos(\theta)-I_5\sin(5\theta+\varphi_5)\cos(\theta)\big) - \\ &-\big(I\sin(\theta)\cos(\theta)+I_5\cos(5\theta+\varphi_5)\sin(\theta)\big)] \\ &= \frac{1}{\sqrt{2}}\big(-I_5\sin(6\theta+\varphi_5)\big) \end{aligned}$$

Furthermore, the d-q currents can be written as:

$$(5)\quad \begin{aligned} i_d &= \frac{1}{\sqrt{2}}\big(I+I_5\cos(6\theta+\varphi_5)\big) \\ i_q &= \frac{1}{\sqrt{2}}\big(0-I_5\sin(6\theta+\varphi_5)\big) \end{aligned}$$

It can be seen in (5) that the fundamental component is found as a continuous component in the d-q frame and the 5th harmonic is found as the 6th harmonic in the d-q frame.

The same calculus can be done also for a system containing the 7th harmonic:

$$(6)\quad \begin{aligned} i_a &= I\cos(\theta) + I_7\cos(7\theta+\varphi_7) \\ i_b &= I\cos\left(\theta-\frac{2\pi}{3}\right) + I_7\cos\left(7\theta-\frac{2\pi}{3}+\varphi_7\right) \\ i_c &= I\cos\left(\theta+\frac{2\pi}{3}\right) + I_7\cos\left(7\theta+\frac{2\pi}{3}+\varphi_7\right) \end{aligned}$$

where I – amplitude of the fundamental, $I_7$ – amplitude of the 7th harmonic, $\theta = \omega t$, $\varphi_7$ – phase angle of the 7th harmonic.

This leads to:

$$(7)\quad \begin{aligned} i_d &= \frac{1}{\sqrt{2}}\big(I+I_7\cos(6\theta+\varphi_7)\big) \\ i_q &= \frac{1}{\sqrt{2}}\big(0+I_7\sin(6\theta+\varphi_7)\big) \end{aligned}$$

Comparing (5) and (7) it can be seen that the 5th and 7th harmonics appear as the 6th harmonic in the d-q frame, the only difference being the sign of the sine component corresponding to the q axis. Thus, by changing the amplitude and phase of a sine wave on the d and q axis, it is possible to obtain a combination of these two harmonics at the output of the active filter.

## 3. THE CONTROLLERS

The controllers used are the classical PI controller, a PI lead-lag controller and a PI+resonant controller.

A simplified model of the system was used for the design of the current controllers.

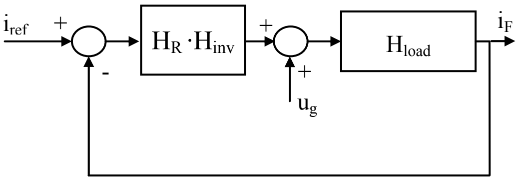


Fig.3. Simplified model

The PI and PI lead-lag controllers were designed using Kessler's symmetrical optimum method [7] and then they were fine-tuned using Matlab's Control System Toolbox and SISOTOOL graphical interface.

A PI+resonant controller was used in order to reduce the influence of the voltage harmonics. The grid voltage $u_g$ is the disturbance in the model presented in Fig.3 and the transfer function in rapport with it is:

$$(8)\quad H_{u_g} = \frac{H_{load}}{1 + H_R H_{inv} H_{load}}$$

The transfer function of the PI+resonant controller used is

$$(9)\quad H_R = K_P + \frac{K_I}{s} + \sum_{h=6,12} K_{Ih} \frac{s}{s^2 + (\omega_0 h)^2}$$

It can be observed in (9) that the transfer function has an extra term $\frac{K_I}{s}$ compared to the P+resonant controller presented in [8], [9], which was used to improve steady-state error. Considering this, the Bode plot of $H_{ug}$ presented in Fig.4 shows large attenuations around the resonant frequencies which are 50Hz, 300Hz and 600Hz, corresponding to the fundamental, and the 5th, 7th, 11th and 13th harmonics in the d-q frame.

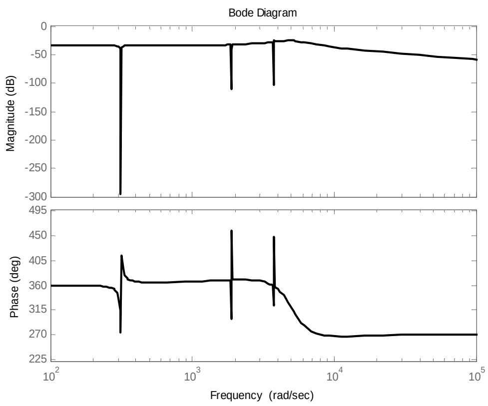


Fig.4. Bode plot for the disturbance transfer function

## 4. EXPERIMENTAL RESULTS

Tests were carried out on a rig built around a 7.5kW Eurotherm Drives 585SV inverter with a R-L filter having L=8.5mH and R=0.8Ω. The control and data acquisition was realised using a dSpace 1104 board. A Matlab/Simulink model was also realised in order to facilitate testing the controllers.

The structure of the rig is presented in fig.5. The variac was used to assure a soft start for the controllers and to avoid over-currents. The isolating transformer was used to charge the capacitor during the start-up procedure. Once the controllers were enabled, the rectifier was disconnected from the mains. The capacitor was maintained charged by a small current on the d axis generated by the PI controller in Fig.2.

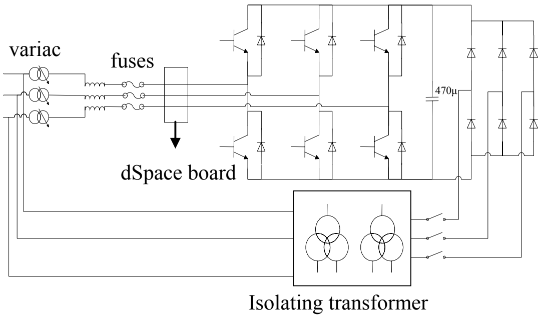


Fig.5. The structure of the test rig

The test signals used were a 2A, 300Hz current reference on the d and q axis, corresponding to 5th or 7th harmonics and a 4A step current reference on the q axis, corresponding to an increase in reactive power [8]. The results obtained for the 300Hz current reference are presented in Fig.6 to 8.

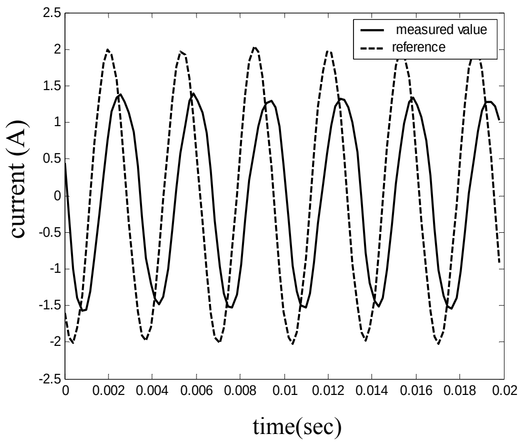


Fig.6. PI controller, current reference 300Hz

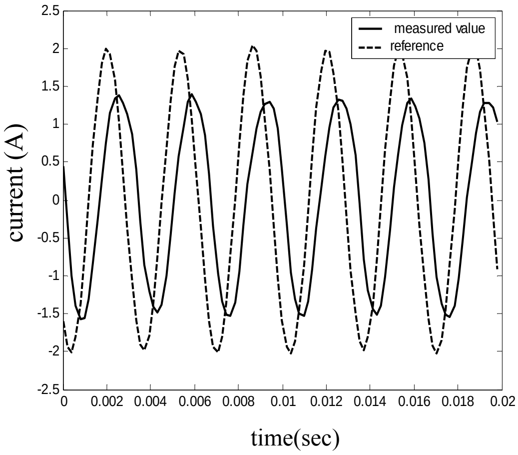


Fig.7. PI lead-lag controller, current reference 300Hz

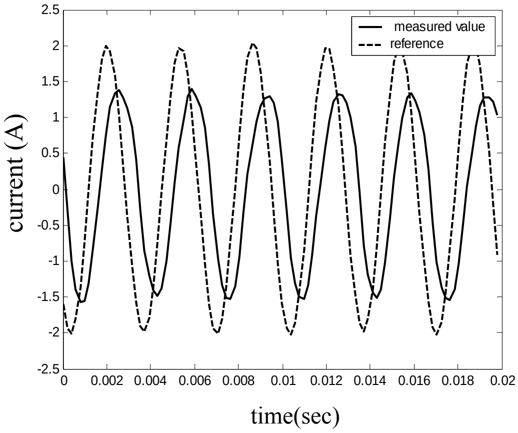


Fig.8. PI+resonant current reference 300Hz

There is a phase shift for all the controllers, and also an error in the amplitude of the output current. The phase and amplitude errors for all the controllers are presented in Table 1.

A 4A step in the q axis current was chosen to test the controllers. This corresponds to an 800VAR increase of the reactive power to be compensated by the active filter [14]. The results are presented in Fig.9 to 11.

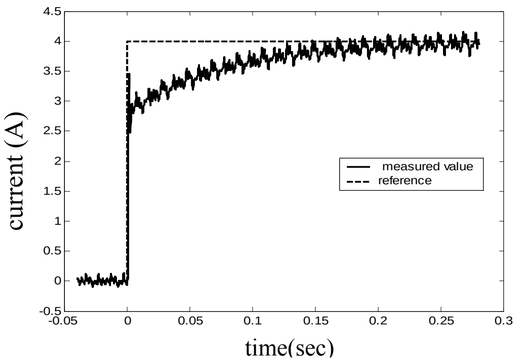


Fig.9. Step response of the PI controller

The rise time of the system when using a PI controller was 0.43ms.

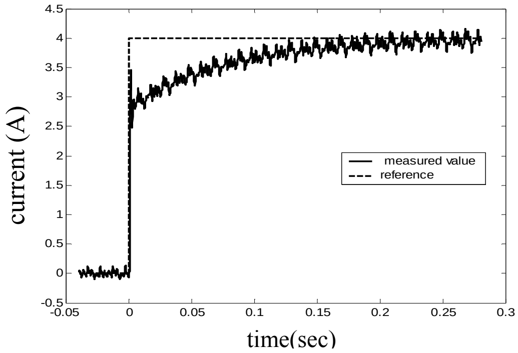


Fig.10. Step response of the PI lead-lag controller

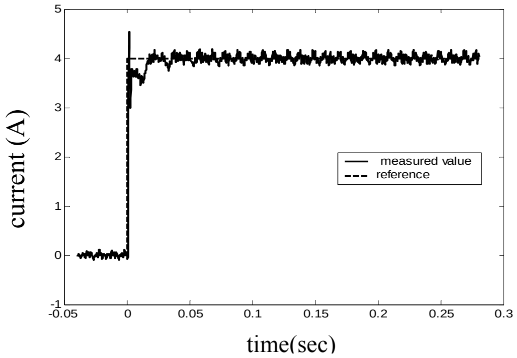


Fig.11. Step response for the PI+resonant controller

The rise time of the system when using a PI lead-lag controller was 0.36ms.

The rise time of the system when using a PI+resonant controller was 0.3ms.

## 5. DATA ANALISYS

The active power filter was used to generate $5^{th}$ and $7^{th}$ harmonics and the measured d and q axis currents were compared to the reference currents. The results for the $5^{th}$ harmonic are presented in Table 1.

Table 1

| | PI | PI lead-lag | PI+resonant |
|---|---|---|---|
| Amplitude error | 26.3% | 19.88% | 5.59% |
| Phase error | 59° | 19.88° | 54.59° |

In order to test the stability of the system the values of the inductance from the filter at the output of the inverter was changed to 5.75mH and 13.75mH. This corresponds to a change of approx. 50% in the impedance of the network.

The results are presented in Table 2, for 5.75mH and 3, for 13.75mH.

Table 2

| | PI | PI lead-lag | PI+resonant |
|---|---|---|---|
| Amplitude error | 19.52% | 14.22% | 3.69% |
| Phase error | 46.25° | 39.54° | 43.73° |

The amplitude and phase error are smaller in this case because by reducing the value of the inductance the time constant of the circuit is reduced.

Table 3

| | PI | PI lead-lag | PI+resonant |
|---|---|---|---|
| Amplitude error | 40.42% | 26.43% | 18.1% |
| Phase error | 74.23° | 58.88° | 71.88° |

An increased value of the inductor leads to a bigger time constant; therefore the dynamic performances of the system are reduced.

The same measurements were carried out for the 7$^{th}$ harmonic. The results are presented in Table 4.

Table 4

| | PI | PI lead-lag | PI+resonant |
|---|---|---|---|
| Amplitude error | 39.6% | 27.24% | 17.1% |
| Phase error | 63.62° | 48.18° | 59.33° |

The amplitude error is bigger than in the case of the 5$^{th}$ harmonic, because the frequency of the reference signal is higher.

The rising time of the step answer allows determining the bandwidth of the system. Considering the relation between the rising time $T_r$ and the bandwidth [12]:

$$(10)\quad BW = \frac{0.35}{T_r}$$

it is possible to synthesise the behaviour of the controllers in table 5.

Table 5

| | PI | PI lead-lag | PI+resonant |
|---|---|---|---|
| Raising time | 0.43ms | 0.36ms | 0.3ms |
| Bandwidth | 750Hz | 1000Hz | 1200Hz |

## 6. CONCLUDING REMARKS

A comparison of different types of controllers was presented in this paper. The tests were carried out using Matlab/Simulink®. An experimental rig was also used for testing with the same conditions for all the controllers.

Based on the measured values, it can be concluded that the PI controller is the less suitable controller for this type of application. Modified versions of the classical PI controller can however lead to better performances.

All the controllers proved to be stable at large variations in the impedance of the network. There is a strong influence of the R-L filter on the performances of the controllers.

Further work will be carried out on the synthesis of the PI+resonant controller. An adaptive control scheme will also be considered.

## 7. REFERENCES

[1] H. Akagi, Y. *Kanazawa*, and A. Nabae, *Instantaneous reactive power compensators comprising switching devices without energy storage components*, IEEE Trans. Ind. App., vol. IA-20, May/June 1984, pp. 625–630
[2] H. Akagi, *New trends in active filters for power conditioning*, IEEE Trans. Ind. App. Vol. 32 no. 6, Nov/Dec. 1996, pp 402 – 408,

[3] L.A. Mohan, J.W. Dixon, R.R. Wallace, *A three phase active power filter operating with fixed switching frequency for reactive power and harmonic compensation*, IEEE Trans. On Ind. El. vol.42, no.4, August 1995, pp 402 – 408

[4] H. Fujita and H. Akagi, *A Practical Approach to Harmonic Compensation in Power Systems-Series Connection of Passive and Active Filters*, IEEE Trans. on Ind. App., Vol. 21, No. 6, Nov/Dec 1991, pp. 1020 – 1025

[5] P. Delarue, J-P Six, F.Ionescu, C. Bogus, *New control method for active power filters,* Proc. ISIE'95, vol.1, pp. 427-432, 1995

[6] S-G Jeong, M-H Woo, *DSP-based active power filter with predictive current control*, Trans. On Ind. El., vol.44, no.3, pp. 329 – 333, 1997

[7] E. Ceanga, L. Protin, C. Nichita, N.A. Cututulis – *Theorie de la commande des systemes*, E. Tehnica, Buc, 2001

[8] D. N. Zmood, D. G. Holmes, *Stationary Frame Current Regulation of PWM Inverters with Zero Steady-State Error* IEEE Trans. on Power Electr., vol. 18, no. 3, May 2003, pp. 814 – 822.

[9] Teodorescu, R., Blaabjerg, F. Borup, U., Liserre, M. *A new control structure for grid-connected LCL PV inverters with zero steady-state error and selective harmonic compensation*, APEC '04. Nineteenth Annual IEEE ,Volume:1, 2004 Pages:580 - 586 Vol.1

[10] Xiaoming Yuan, Merk, W., Stemmler, H., Allmeling, J., *Stationary-frame generalized integrators for current control of active power filters with zero steady-state error for current harmonics of concern under unbalanced and distorted operating conditions* IEEE Trans. On. Ind. Appl.,Volume: 38 , no 2 , March-April 2002 pp:523 - 532

[11] M. Kazmierkowski, R.Krishnan, F.Blaabjerg, *Control in Power Electronics. Selected Problems,* Academic Press 2002, ISBN 0-12-402772-5.

[12] *** - *Control System Toolbox. User's guide*, Mathworks, 2000

[13] R. Burns, *Advanced Control Engineering,* Butterworth-Heineman, 2001, ISBN 0-7506 51008

[14] J.Arilaga, N. Watson, *Power Systems Harmonics,*, J. Wiley&Sons., 2003, ISBN 0-470-85129-5